Molecular Crystals and Liquid Crystals Science and Technology. Section A. Molecular Crystals and Liquid Crystals
Publication details, including instructions for authors and subscription information:
http://www.tandfonline.com/loi/gmcl19

Description of the Normal-Roll Instability in Nematic Liquid Crystals Using a Generalized Potential Functional

Alexander M. L. Nip [a] & J. A. Tuszyński [a]
[a] Department of Physics, University of Alberta Edmonton, Alberta, Canada, T6G 2J1
Version of record first published: 04 Oct 2006.

To cite this article: Alexander M. L. Nip & J. A. Tuszyński (1996): Description of the Normal-Roll Instability in Nematic Liquid Crystals Using a Generalized Potential Functional, Molecular Crystals and Liquid Crystals Science and Technology. Section A. Molecular Crystals and Liquid Crystals, 289:1, 103-125

To link to this article: http://dx.doi.org/10.1080/10587259608042316

Mol. Cryst. Liq. Cryst., 1996, Vol. 289, pp. 103–125
Reprints available directly from the publisher
Photocopying permitted by license only

Description of the Normal-Roll Instability in Nematic Liquid Crystals Using a Generalized Potential Functional

ALEXANDER M. L. NIP and J. A. TUSZYŃSKI

Department of Physics, University of Alberta
Edmonton, Alberta, Canada T6G 2J1

(Received in final form 22 November 1995)

We provide an example for the use of a generalized potential functional in a nonequilibrium pattern forming process by re-examining the critical behavior of the normal rolls in an electrically-driven nematic cell. We show that the viscous torque due to the flow on the director can be derived from a functional and consequently convert the equation of state to a gradient form. The standard hydrodynamic together with Maxwell's equations are used to determine an explicit form of the field variables. First order nonlinear corrections to the linear solutions are obtained using a technique similar to the ε-expansions. Upon minimization of the nonequilibrium potential with respect to the state parameters, we construct a bifurcation diagram for a continuous transtition and reproduce the observed $\varepsilon^{1/2}$ power-law dependence. A criterion for the formation of the normal rolls via a discontinuous transition is also given within the model.

Keywords: Nematic liquid crystal; rolls; instability

PACS numbers: 47.20.Ky, 47.25.Ae, 47.65.+a

1. INTRODUCTION

Convection caused by electroactivities in nematic liquid crystal thin films has been an object of intensive experimental and theoretical studies [1–12] mainly due to these systems' intrinsically large aspect ratio which makes them ideal candidates for the investigation of pattern formation. Under proper experimental conditions (see section II), a thin layer of a nematic liquid crystal can be excited by an *a. c.* electric field, at appropriate

frequency values, to produce a sequence of convective patterns similar to those observed in the Rayleigh-Bénard convection of the isotropic fluids [13]. This transition sequence includes the familiar **normal rolls**, the **oblique rolls**, the **skewed varicose** and the **bimodal** patterns [9]. While many of these convective pattern formation phenomena have been observed and quantified experimentally, parallel theoretical investigations have progressed too, albeit at a somewhat slower rate. Due to the complexity of the equations of motion involved, accurate predictions have been provided mainly by the linear theory at the transition threshold [1, 3, 4, 14] and, for a very limited range above the primary transition line, good qualitative descriptions have become available only thorugh a weakly nonlinear analysis [5, 15].

As revealed by an experiment performed by Rasenat *et al.* [10], slightly above the transition from the rest state to the normal rolls, the nematic layer exhibits a power-law behavior: the modulational amplitude of the molecular alignment θ_0 increases as a square root of the reduced voltage $\varepsilon = (V^2 - V_c^2)/V_c^2$ (also regarded as an infinitesimal bifurcation parameter) where V and V_c are the applied root-mean-sqare voltage and the *rms* threshold voltage of the transition, respectively. Unfortunately, this critical behavior cannot be explained by the linear theory. The only model that has produced satisfactory (qualitative) results so far in this regime is the amplitude description [5, 15] where each of the solutions is first expanded in fractional powers of ε as:

$$u(x, y, z, t) = \varepsilon^{1/2}[u_0(x, y, z, t) + \varepsilon^{1/2} u_1(x, y, z, t) + \varepsilon u_2(x, y, z, t) + \cdots]. \quad (1.1)$$

Rather disappointingly, the leading order in the above expansion is a priori chosen so as to achieve detailed balance in the equations of state. The critical behavior of θ_0 is therefore not a direct result of the model. To our knowledge, this critical phenomenon still remains unresolved theoretically.

However, the amplitude description has provided us with an alternate view of the problem. Using the technique of the multiscale analysis (introducing the slow variables $X = \varepsilon^{1/2}x$, $Y = \varepsilon^{1/2}y$ and $T = \varepsilon t$) coupled with the neutral solutions, u_0, of the form

$$u_0 = [A(X, Y, T)e^{i\vec{q}_c \cdot \vec{x}} \pm c.c.]\bar{u}_0(z, t), \quad (1.2)$$

Bondenschatz *et al.* [5] were able to demonstrate that the complex amplitude $A(X, Y, T)$ satisfies the evolution equation

$$T_0 \partial_T A = [\xi_\parallel^2 \partial_X^2 + \xi_\perp^2 \partial_Y^2 + 1 - |A|^2]A \quad (1.3)$$

which, in its dimensionless form, is mathematically equivalent to the time-dependent Landau-Ginzburg equation (TDLG) [16, 17], describing the time relaxation of the (non-conserved) order parameter (A in this case) towards its stationary state. TDLG is not only known to produce good qualitative predictions for many pattern-forming systems involving fluids near the first transition threshold [18–22], it has also found applications in many other nonequilibrium processes [23] including second-order phase transition of a junction laser [24], propagation of a two-phase interface [25] and superconductivity [26–28]. This universality leads us yet to another important result. It has been pointed out, in a recent review by Cross and Hohenberg [29], that although in general no free energy or Lyapunov potential can be defined for nonequilibrium systems, those in which the dynamics of the order parameter is prescribed by TDLG remain notable exceptions. In fact, TDLG can be readily converted to the gradient form

$$\frac{\partial \psi}{\partial t} = -\Gamma \frac{\delta G}{\delta \psi^*} \tag{1.4}$$

with Γ being a positive kinetic coefficient and G a potential functional of the complex order parameter ψ and ψ^*. Moreover, the functional G can be shown to be equivalent to a Lyapunov function. The stationary state of the system is therefore determined by the minimum of G.

In order to describe the critical behavior of θ_0 near the threshold, we seek in this paper an alternative way of constructing a nonequilibrium generalized potential functional for the nematic system. Having said that, the functional G from the amplitude equation is of little use to us since the $\varepsilon^{1/2}$ power-law is already the underlying assumption of the model. The method we adopt here is similar to that proposed by Graham and Tél [30, 31]. We choose, as our order parameter, $\theta = \theta_0 f(r)$ where r, known as the normalized domain spacing, is the ratio of the width of the normal rolls ($\lambda/2$) to the thickness (d) of the nematic sample and we rewrite the equation of state — the torque-balance equation — in a gradient form. While the dynamics is determined by the usual hydrodynamic equations and Maxwell's equations, the stationary values of the order parameter, and therefore those of θ_0 and r, are determined by minimizing the nonequilibrium potential, leading to a bifurcation diagram for the rest-state to normal rolls transition.

2. NORMAL-ROLL INSTABILITY

Our analysis is focused on a thin layer of a nematic liquid crystal which has a negative dielectric anisotropy $\Delta\varepsilon = \varepsilon_{\parallel} - \varepsilon_{\perp}$ but a positive conduction anisotropy $\Delta\sigma = \sigma_{\parallel} - \sigma_{\perp}$. The layer is sandwiched between two parallel glass plates specially treated so as to impose a uniform alignment parallel to the glass surfaces (the x-direction) in the unperturbed configuration. A spatially-uniform *a.c.* electric field $E_0 \cos(\omega t)$ is applied along the normal axis of the nematic layer (the z-direction) to provide an external source of energy.

According to the Helfrich scenario [1–3], the onset of normal-roll instability is mainly due to the "victory" of the driving torques in their "battle" against the restoring torques. At the initial stage, the uniform state of the nematic cell is absolutely stable. Any perturbation in the director field will inevitably raise the deformation energy and lead to a restoring torque that will bring the system back to its uniform state. The applied electric field further contributes to the stability of the uniform state. Since the dielectric anistropy of the liquid crystal is negative, the molecules tend to align themselves orthogonally to the electric field. As a result, a dielectric torque is present to guard against any distortion in the director thereby re-enforcing the uniform state. The origin of the instability can be traced to the presence of impurity ions in any electroconvective experiments involving liquid crystals. Once the electric field is applied, a bend deformation in the director field, no matter how small, causes the impurity ions to separate into postive and negative charges. Dragged by the electric field, these charges accumulate in the high curvature regions of the director field, alternating in polarity along the x-direction. This charge accumulation has two effects. First, it sets up an additional electric field within the sample. While the z-component of this field helps to maintain the uniform state, the other orthogonal component is destabilizing, causing the director to deviate. Secondly, in response to the electric field, the motion of these ionic charges stirs up a cellular flow and the flow in turn exerts destabilizing hydrodynamic torques on the director. The destabilizing torques are weak at sufficiently low voltages and so they do not pose a threat to the stability of the uniform state at the early stage. However, they increase with the applied voltage and begin to outbalance the restoring torques as the threshold voltage is approached. At the transition point, the state of parallel alignment becomes unstable; a new stationary structure whose director is bent periodically in the x-direction emerges as a set of parallel straight rolls.

3. A GENERALIZED POTENTIAL FUNCTIONAL

Therefore, based on the above description, we see that the equation that determines the stability of the system is the sum-of-torques equation, which, for stationary states, is written as

$$\tau_d + \tau_e + \tau_v = 0 \tag{3.1}$$

where τ_d, τ_e and τ_v correspond respectively to the deformation, the dielectric and the viscous torques. To obtain a generalized nonequilibrium potential functional F, the above equation must be converted to a gradient form, or equivalently speaking, to the time-independent Landau-Ginzburg equation:

$$\frac{\delta F}{\delta \theta} = 0. \tag{3.2}$$

Then, the potential F must consist of three contributing terms with each term corresponding to a functional from which the associated torque is derived. Accordingly, we denote F as

$$F = F_d + F_e + F_v \tag{3.3}$$

where the subscripts carry the same meaning as those appearing in Eq. (3.1).

The first two terms on the right hand side of the above equation have been exhaustively discussed in the literature on this topic [3, 4, 14, 32, 33]. The deformation energy F_d, also known as the Frank deformation energy [32, 33], is in turn a sum of three elementary deformation energies:

$$F_d = \int \frac{1}{2} k_{11} (\vec{\nabla} \cdot \vec{n})^2 + \frac{1}{2} k_{22} [\vec{n} \cdot (\vec{\nabla} \times \vec{n})]^2 + \frac{1}{2} k_{33} [\vec{n} \times (\vec{\nabla} \times \vec{n})]^2 \, dV \tag{3.4}$$

where $\vec{n}$ is the director field and k's are the positive elastic constants. These elementary deformations of the director are respectively the splay, the twist and the bend. However, not all of these terms are necessary in analyzing the formation of normal rolls. Since it has been observed that [8, 9] the director field of the normal rolls is "bent" periodically only in the x-direction and has no y-dependence at all, the twist deformation is not present. For this reason, we shall omit the second integrand in Eq. (3.4) in the rest of the analysis. The dielectric energy describes the coupling between the director

and the total electric field. Similarly to the energy of a ferromagnet in the presence of a magnetic field, the dielectric energy for the nematic is written in terms of the dot product of its internal degrees of freedom and the external field [32]:

$$F_E = -\int \frac{\Delta\varepsilon}{2}(\vec{n}\cdot\vec{E})^2\, dV \tag{3.5}$$

where the square is there to reflect the symmetry requirement that the two ends of the molecule are not distinguishable.

Since the interaction between the director and the fluid flow represents a source of dissipation, the viscous torque τ_v in principle is not derivable from a thermodynamic (equilibrium) potential. However, this is not to say that τ_v cannot be expressed in the gradient form $\tau_v = \delta F_v/\delta\theta$ with F_v being an effective nonequilibrium potential. In fact, F_v can be found by carefully examining the analytic expression for τ_v obtained from the consideration of entropy production. According to de Gennes [32], the fluid flow exerts the counter-torque

$$\tau_v = -(\vec{n}\times\vec{h})_y \tag{3.6}$$

$$= \frac{1}{2}(\alpha_3-\alpha_2)\left(\frac{\partial v_x}{\partial z}-\frac{\partial v_z}{\partial x}\right) - \frac{1}{2}(\alpha_2+\alpha_3)\left[\left(\frac{\partial v_x}{\partial x}-\frac{\partial v_z}{\partial z}\right)\sin(2\theta) - \left(\frac{\partial v_x}{\partial z}+\frac{\partial v_z}{\partial x}\right)\cos(2\theta)\right] \tag{3.7}$$

on the director. The field $\vec{h}$ is known as the molecular field and is a linear combination of the time rate of change of the director field with respect to the background flow and the velocity gradient. It represents, in this case, an internal destabilizing field which causes the director to deviate from its uniform configuration. In the above torque expression, α's are the viscous coefficients; v's are the velocity components and θ is the tilt angle of the director made with respect to the horizontal (x-) axis. In accordance with the experimental observations [8, 9], we have assumed that the director field has a vanishing y-component i.e. $\vec{n} = (\cos\theta, 0, \sin\theta)$. We can deduce the form of the nonequilibrium potential by seeking a functional that produces the correct viscous torque (3.7). Examining Eq. (3.6), we could construct this functional naively by integrating the dot product of the internal degrees of freedom and the destabilizing field, analogously to the energy of an electric

dipole in the presence of an electric field. If we assume

$$F_v = \int \frac{1}{2}(\vec{n}\cdot\vec{h})\,dV, \tag{3.8}$$

it is easy to show that the corresponding torque ($\tau_v = \delta F_v/\delta\theta$) is given by

$$\tau_v = -\frac{1}{2}(\alpha_2+\alpha_3)\left[\left(\frac{\partial v_x}{\partial x}-\frac{\partial v_z}{\partial z}\right)\sin(2\theta)-\left(\frac{\partial v_x}{\partial z}+\frac{\partial v_z}{\partial x}\right)\cos(2\theta)\right]. \tag{3.9}$$

Clearly, this torque corresponds to only a portion of the complete expression (3.7). Therefore, the dot product alone is not sufficient. We have discovered that the complete viscous torque can be reproduced if we add to the dot product an extra term so that the functional takes the following form:

$$F_v = \int -\left(\frac{\alpha_3-\alpha_2}{2}\right)\vec{v}\cdot[(\vec{\nabla}\cdot\vec{n})\vec{n}+\vec{n}\times(\vec{\nabla}\times\vec{n})]+\frac{1}{2}(\vec{n}\cdot\vec{h})\,dV. \tag{3.10}$$

At the first sight, it appears that F_v is not time-reversal invariant. However, since we are dealing with a stationary (steady) state, the velocity field is constant in time. Thus, the time-reversal symmetry is preserved. It should also be noted that this energy density has the correct dimension and does satisfy the necessary symmetry requirements of a nematic liquid crystal. We could insist on writing F_v as an integral of a dot product. However, doing so would require that a new destabilizing field be introduced as follows:

$$F_v = -\int \frac{1}{2}(\vec{n}\cdot\vec{\mathscr{H}})\,dV \tag{3.11}$$

where the new field $\mathscr{H}$ is written as

$$\vec{\mathscr{H}} = (\alpha_3-\alpha_2)[(\vec{\nabla}\cdot\vec{n})\vec{v}+(\vec{\nabla}\times\vec{n})\times\vec{v}]-\vec{h} \tag{3.12}$$

and is referred to as the generalized molecular field here. It is not difficult to see that a parallel alignment of $\vec{n}$ with the field $\vec{\mathscr{H}}$ is energetically favorable.

Our nonequilibrium potential functional for the nematic cell can now be fully assembled in the equation below

$$F = \int \left\{ \frac{1}{2} k_{11} (\vec{\nabla} \cdot \vec{n})^2 + \frac{1}{2} k_{33} [\vec{n} \times (\vec{\nabla} \times \vec{n})]^2 - \frac{\Delta\varepsilon}{2} (\vec{n} \cdot \vec{E})^2 - \frac{1}{2} (\vec{n} \cdot \vec{\mathscr{H}}) \right\} dV. \tag{3.13}$$

In addition to the director's vanishing y-component and its being independent of y, experiments [8, 9] have also demonstrated that the velocity field in the normal rolls does not have an axial component and that it merely circulates about the roll axes. We can infer from these observations that the total electric field must be parallel to the x–z plane and be independent of y. Therefore, we can formally treat this transition as a two-dimensional problem. In this regard, the above potential functional is dependent on five field variables (degrees of freedom), namely, the tilt angle of the director θ, the velocity components v_x and v_z and the electric field components E_x and E_z.

4. THE NONLINEAR SOLUTIONS

Although we can use the above potential functional to obtain the stationary values of the state parameters θ_0 and r, we can only do so if we know the explicit form of the field variables involved. Since the potential cannot determine the dynamics of the system, we turn to the hydrodynamic and Maxwell's equations. In order to simplify our analysis, we first assume that the nematic liquid crystal in question is incompressible so that the mass density ρ is an invariant and the velocity field becomes divergenceless as a result:

$$\vec{\nabla} \cdot \vec{v} = 0. \tag{4.1}$$

Secondly, we assume that the velocity field is sufficiently weak so that convective terms such as $(\vec{v} \cdot \vec{\nabla}) f_i$ stands for an arbitrary field component, can be safely ignored wherever they appear. Under these assumptions, the equations that describe the fluid motion due to the applied forces are the hydrodynamic equations of the form

$$\rho \frac{\partial v_\beta}{\partial t} = \partial_\alpha \sigma_{\alpha\beta} + q E_\beta \tag{4.2}$$

where summation over repeated indices has been assumed. In these equations, the terms qE_β express the body force that arises from the dragging of the impurity ions by the electric field and the tensor σ is the total stress tensor [32, 34–36].

These equations alone however do not suffice to determine the physically realizable states of the system; to describe the dielectric response of the liquid crystal, they must be supplemented by Maxwell's equations. In the absence of magnetic fields, Faraday's law (in MKSA units) takes on the simple form

$$\vec{\nabla} \times \vec{E} = 0. \tag{4.3}$$

The remaining Maxwell equations can then be combined to yield the conservation of charge equation:

$$\vec{\nabla} \cdot \vec{J} + \frac{\partial q}{\partial t} = 0. \tag{4.4}$$

Altogether, (4.1), (4.2), (4.3) and (4.4) constitute a set of equations which suffice to determine the explicit form of the necessary field variables. These equations are in principle solvable; however, the presence of nonlinearities precludes the use of exact methods. In the past, these equations have been linearized and their linear solutions have been readily obtained. It is now known that analytical solutions exist only for the semi-rigid boundary conditions [14, 37] which mean that, except for a non-zero but very small tangential velocity, all other field components are required to vanish at the vertical boundaries ($z = \pm d/2$). Under these conditions, the linear solutions are all found to be proportional to a small-scale parameter θ_0:

$$\theta = \sin(px)\cos(qz)\,\theta_0 \tag{4.5}$$

$$E_x = \bar{E}_{x1}(t)\sin(px)\cos(qz)\,\theta_0 \tag{4.6}$$

$$E_z = \frac{q}{p}\bar{E}_{x1}(t)\cos(px)\sin(qz)\,\theta_0 \tag{4.7}$$

$$v_x = \bar{v}_{x1}\sin(px)\sin(qz)\,\theta_0 \tag{4.8}$$

$$v_z = \frac{p}{q}\bar{v}_{x1}\cos(px)\cos(qz)\,\theta_0 \tag{4.9}$$

where $p = 2\pi/\lambda$ and $q = \pi/d$ are the spatial frequencies of the normal rolls in the horizontal (x-) and the vertical (z-) directions, respectively. Explicit expressions for the coefficeints $\bar{E}_{x1}(t)$ and $\bar{v}_{x1}$ can be found in the Appendix. According to Eq. (4.5), θ_0 can be interpreted as the modulational amplitude of the director. It is not difficult to see that this amplitude must be dependent upon the reduced voltage $\varepsilon = (V^2 - V_c^2)/V_c^2$. After all, the tilt angle of the director field must vanish as the voltage approaches the threshold value. Unfortunately, the linear theory is not able to describe this voltage dependence, since, upon substitution, θ_0 drops out of the equations of motion completely.

This voltage dependence can nevertheless be determined by using the nonequilibrium potential functional obtained earlier. Since we are only interested in the immediate neighborhood of the transition point, the scale on which the bifurcation takes place is infinitesimally small. This scale is presumbly on the order of θ_0. Consequently, we can expand each field component as an asymptotic series in θ_0 as follows:

$$\varphi = \varphi_1\theta_0 + \varphi_2\theta_0^2 + \cdots \tag{4.10}$$

where the first-order coefficient φ_1 corresponds naturally to the linear solution discussed above. Then, substituting Eq. (4.10) into the equations (4.1)–(4.4) and collecting like order terms, we obtain sets of simultaneous equations, each of which is associated with a different order of θ_0. Solving these sets of equations in a consecutive manner starting from the lowest order set, one finds that the first-order set produces the linear solutions, the second-order set produces the first nonlinear corrections (i.e. the φ_2's) and so on. We can continue to solve these sets of equations for as many nonlinear corrections as we see appropriate. Then, upon substitution of the series solutions (4.10), the nonequilibrium potential functional (3.13) can be shown to form an asymptotic series in θ_0, with the coefficients dependent on the normalized domain spacing of the normal rolls $r = q/p$, the applied voltage V as well as the applied field frequency ω. Consequently, the stationary values of r and θ_0 at each voltage and frequency can be determined by means of minimization.

Just as the linear solutions are all composed of the fundamental harmonics, the second-order coefficients in the series solutions are found, through the first nonlinear balance, to consist of the second-order harmonics:

$$\theta_2 = \frac{q}{4p}\sin(2px)\sin(2qz) \tag{4.11}$$

$$E_{x2} = \bar{E}_{x2}(t)\sin(2px)\sin(2qz) \tag{4.12}$$

$$E_{z2} = -\frac{q}{p}\bar{E}_{x2}(t)\cos(2px)\cos(2qz) + \bar{E}_{z2}(t)\cos(2qz) \tag{4.13}$$

$$v_{x2} = \bar{v}_{x2}\sin(2px)\cos(2qz) \tag{4.14}$$

$$v_{z2} = -\frac{p}{q}\bar{v}_{x2}\cos(2px)\sin(2qz) \tag{4.15}$$

where explicit expressions for the coefficients $\bar{E}_{x2}(t)$, $\bar{E}_{z2}(t)$ and $\bar{v}_{x2}$ are listed separately in the Appendix. Although this is only the first step beyond the linear approximation, the equations and the algebra involved are already very complex. Going beyond this order of approximation becomes exceedingly cumbersome. For this reason, we shall restrict ourselves to expansions up to the second-order in θ_0 only. Duing so will, no doubt, affect the accuracy of our final results. One foreseen disadvantage is that the high order coefficients in the expansion of the potential would be inexact and this could compromise the validity of the expansion over an extended range in the $\theta_0 - r$ parameter plane. This approximation is nevertheless justifiable in a close proximity of the transition point since r is approximately 1 and θ_0 is very close to 0 near criticality. We shall demonstrate that, in spite of its approximate nature, the model produces results which compare very well with experiment.

5. DIRECT BIFURCATION

Proceeding in the manner described above, we insert the series solutions into the nonequilibrium potential (3.13) and collect terms of like orders in θ_0. It turns out that odd order terms in θ_0 vanish identically; hence, the nonequilibrium potential per unit cell per cycle $\mathscr{F}$ is an even series in θ_0:

$$\mathscr{F} = C_2(r; V, \omega)\theta_0^2 + C_4(r; V, \omega)\theta_0^4 + \cdots \tag{5.1}$$

where the second- and the fourth-order coefficients are given respectively as

$$C_2 = \frac{\pi^2}{8d^2}\left(k_1 + \frac{k_3}{r^2}\right) + \frac{V^2}{d^2}\left[\frac{a(\alpha_2 - \alpha_3 r^2)}{4(\omega^2\tau^2 + 1)\xi} + \frac{\Delta\varepsilon(2b - g)}{8g}\right], \tag{5.2}$$

$$C_4 = \frac{\pi^2}{128d^2}\left[k_1\left(4r^2 + \frac{3}{r^2} - 9\right) + k_3\left(13 - \frac{3}{r^2}\right)\right]$$

$$-\frac{V^2}{8d^2}\left\{\frac{\Delta\varepsilon r^2}{16g^2}\left[b^2+a^2\omega^2+4(A_2-A_1\tau\omega^2)+g^2-\frac{2S_1}{g}\right]\right.$$

$$-\frac{3\Delta\varepsilon}{16g^2}\left[3b^2-4bg+g^2+3a^2\omega^2+\frac{4S_2}{3g(\sigma_\perp^2+\varepsilon_\perp^2\omega^2)}\right]$$

$$+\frac{a}{8(\tau^2\omega^2+1)\xi}[(\alpha_2+\alpha_3)(3+12\bar{v}_{x2}r-5r^2-4\bar{v}_{x2}r^3)$$

$$\left.-4\bar{v}_{x2}(\alpha_3-\alpha_2)r(r^2+1)]\right\} \tag{5.3}$$

with

$$S_1=b(2A_2-bg+2g^2)+a(2A_1-ag)\omega^2+2\tau\omega^2(aA_2-bA_1), \tag{5.4}$$

$$S_2=g[a\omega^2(A_2\varepsilon_\perp+A_1\sigma_\perp)+(b-g)(A_2\sigma_\perp-A_1\omega^2\varepsilon_\perp)]$$

$$+r^2(\sigma_\perp^2+\varepsilon_\perp^2\omega^2)[a\omega^2(A_2\tau+A_1)+(b-g)(A_2-A_1\tau\omega^2)], \tag{5.5}$$

The interested reader is referred to the Appendix for definitions of the parameters A_1, A_2, a, b, g, τ and ξ used in the above expressions. Since the phenomenon involves a continuous (second-order) phase transition, we expect $\mathscr{F}$ to bifurcate from a single well to a double well form as the applied voltage exceeds its threshold value V_c. Consequently, the essential physics is captured by the first two terms in the expansion. For simplicity, we shall therefore truncate the expansion at the fourth-order term as

$$\mathscr{F}=C_2\theta_0^2+C_4\theta_0^4. \tag{5.6}$$

Considering the complexity of this mean potential, we believe that a global search for the minimum may not be feasible either analytically or numerically. We have thus decided to limit the search region to a subset consistent with experimental observations and a stability criterion and to resort to numerical techniques for the remainder of the analysis.

As we have pointed out previsouly, θ_0 is close to zero and r is roughly unity in the neighborhood of the transition point. Experimental observations [9] have further indicated that r decreases slightly as the voltage continues to increase. It is therefore reasonable to limit our search region first to $[0, 1] \times [0, 1]$ in the θ_0-r parameter plane. In addition to these experimental indications, for stability reasons, the fourth-order coefficient must always be

positive in the region of our search. Using the standad material parameters for the room temperature nematic liquid crystal MBBA (see Tab. I), in Figure 1, we display typical plots of C_4 at the reduced frequency of $\omega' = \omega\varepsilon_\parallel/\sigma_\parallel = 0.5$ for three different values of the applied *rms* voltage. We readily note that the coefficient becomes negative in the central region of the graph. This anomaly could be caused by the inexactness due to the truncation of the series solutions as pointed out earlier. It could also mean the presence of a metastable state, which is allowed to exist when the fourth-order coefficient becomes negative while the sixth-order coefficient is positive. To prove that a metastable state actually exists in our system, we would have to calculate the sixth-order coefficient explicitly and this is beyond the scope of our analysis. It will, therefore, be feasible to limit our search interval of r to the range $[0, \delta)$ where δ is the critical point at which C_4 first crosses the r-axis in Figure 1.

We again fix the reduced field frequency ω' at 0.5 and plot the second-order coefficient C_2 as a function of r for three different values of the applied voltage in Figure 2. Evidently, so long as the voltage is below a critical value, the coefficient is positive everywhere. Since C_4 is also positive within the region of our search, this indicates that a single well with its minimum located somewhere on the r-axis is present in the potential. The corresponding stationary state ($\theta_0 = 0$) can therefore be interpreted as the rest-state of the nematic cell. However, as shown in the corresponding figure, once the voltage exceeds its critical value even slightly, the coefficient becomes negative over a small range of r meaning that the single well in the potential has split into two wells and these wells have drifted away from the r-axis. Although there are now two equivalent minima, one with $\theta_0 > 0$ and the other with $\theta_0 < 0$, physical constraints on θ_0 demand that the minimum located in the positive quadrant of the parameter plane corresponds to the true stationary state of the system. Since this state has a non-zero θ_0, it corresponds very naturally to the normal rolls.

It is now clear that the bifurcation must take place at the point where the C_2 curve in Figure 2 just touches the r-axis. Setting C_2 to zero, we can re-arrange the equation and express the *rms* voltage as a function of r and ω as follows:

$$V_{rms}^2 = \frac{\pi^2}{r^2}(k_1 r^2 + k_3)(\tau^2\omega^2 + 1)\left\{\frac{2(\alpha_3 r^2 - \alpha_2)(\sigma_\parallel\varepsilon_\perp - \varepsilon_\parallel\sigma_\perp)(r^2+1)}{(\sigma_\parallel + \sigma_\perp r^2)\xi}\right.$$

$$\left. + \Delta\varepsilon\left[\frac{\sigma_\perp(r^2+2) - \sigma_\parallel}{\sigma_\parallel + \sigma_\perp r^2} + \frac{\tau^2\omega^2[\varepsilon_\perp(r^2+2) - \varepsilon_\parallel]}{\varepsilon_\parallel + \varepsilon_\perp r^2}\right]\right\}^{-1}. \tag{5.7}$$

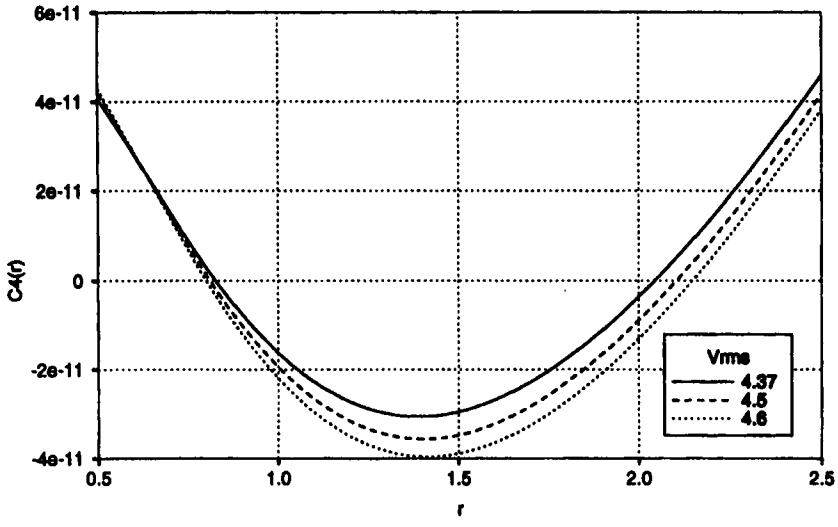

FIGURE 1 The fourth-order coefficient C_4 plotted as a function of the normalized domain spacing r at $\omega' = 0.5$ for three different values of V.

TABLE I Physical parameters for the room temperature nematic liquid crystal MBBA (following reference [5])

parameter	*value*
k_1,	6.10×10^{-12} N
k_3	7.25×10^{-12} N
α_1	6.5×10^{-3} Kg/m/s
α_2	-77.5×10^{-3} Kg/m/s
α_3	-1.2×10^{-3} Kg/m/s
α_4	83×10^{-3} Kg/m/s
α_5	46×10^{-3} Kg/m/s
α_6	-35×10^{-3} Kg/m/s
$\varepsilon_\parallel$	$4.72 \times \varepsilon_0$
$\varepsilon_\perp$	$5.25 \times \varepsilon_0$
$\sigma_\parallel/\sigma_\perp$	≈ 1.5

Except for some numerical factors, this equation is identical in form to the compatibility condition derived in the linear theory [4, 14]. To obtain the transition curve for the purpose of comparing theory with experiment, we minimize the above *rms* voltage numerically with respect to r over a range of frequency. If we choose to use the non-standard value 1.15 for the conductivity ratio $\sigma_\parallel/\sigma_\perp$, then the resultant transition curve as shown in Figure 3 compares very favorably with the experimental measurements [6]. To superimpose the experimental data onto Figure 3, we have taken $\sigma_\parallel$ to

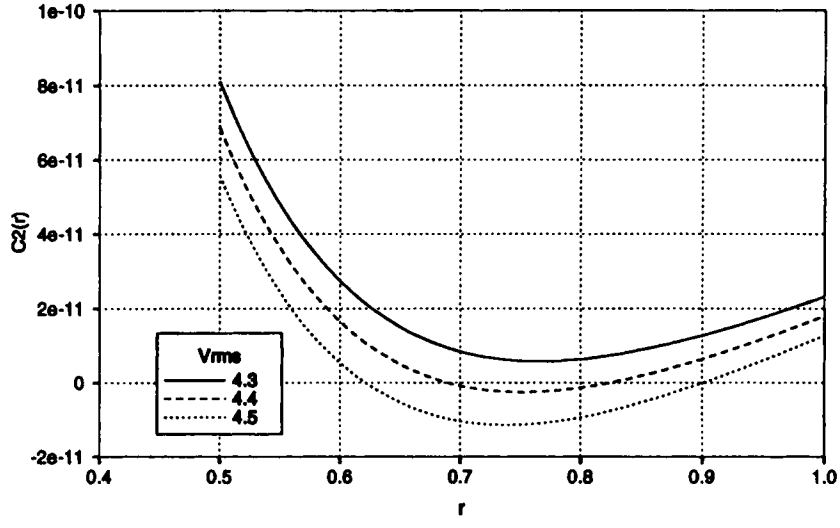

FIGURE 2 The second-order coefficient C_2 plotted as a function of the normalized domain spacing r at $\omega' = 0.5$ for three different values of V.

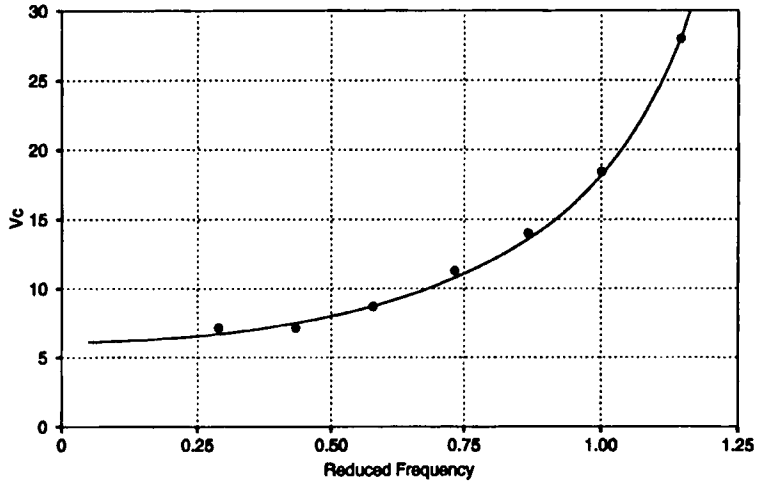

FIGURE 3 The transition line for the rest-state to normal-roll transition. The solid line is calculated at $\sigma_\parallel/\sigma_\perp = 1.15$; the dots represent the experimental measurements taken from reference [6].

be $1.8450 \times 10^{-8}\Omega^{-1}\mathrm{m}^{-1}$ so that the experimental point on the extreme right of the graph coincides with the theoretical transition curve.

We finally turn our attention to the bifurcation diagram for the continuous rest-state to normal rolls transition. The diagram can be constructed by

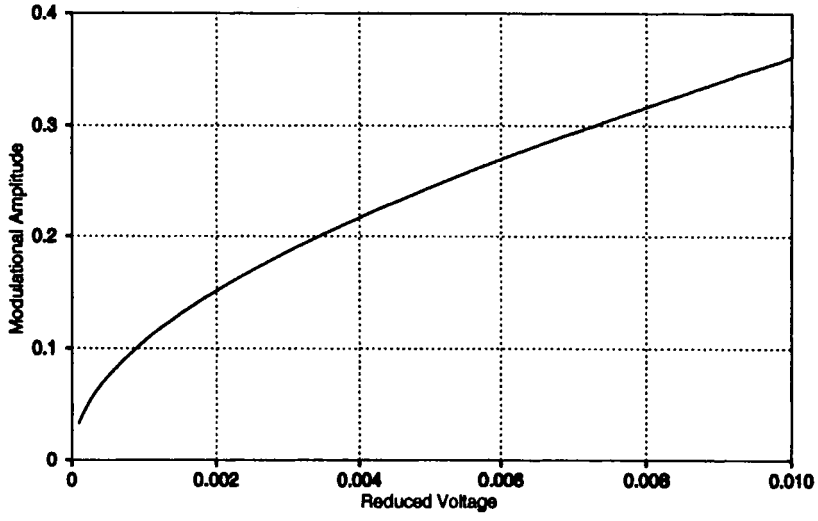

FIGURE 4 Bifurcation diagram for θ_0 near criticality.

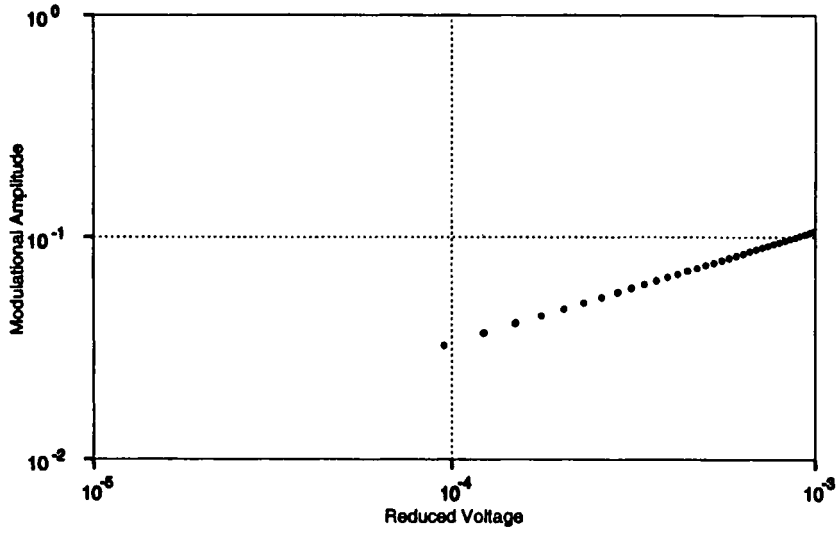

FIGURE 5 A log-log plot of the bifurcation diagram for θ_0.

minimizing $\mathscr{F}$ with respect to the state parameters r and θ_0. With all the physical parameters for MBBA taken directly from Table I, we have employed a multidimensional minimization algorithm [38] to minimize $\mathscr{F}$ at $\omega' = 0.5$ for a range of V slightly above the threshold voltage. For the conductivity $\sigma_{\parallel}$, we have chosen the value $1.1895 \times 10^{-8}\Omega^{-1}\mathrm{m}^{-1}$ so that

the reduced frequency corresponds to the actual frequency $f = 22.65$ Hz where a continuous transition has indeed been observed [6–8]. In Figure 4, we plot the amplitude θ_0 as a function of the reduced voltage ε. We can see that θ_0 does increase nonlinearly with ε near criticality. As for the question whether it has the observed power-law behavior, we turn to the log-log plot as shown in Figure 5 where θ_0 is seen to increase with ε according to

$$\theta_0 = \mathscr{A}\varepsilon^{\beta} \tag{5.8}$$

where the critical amplitude $\mathscr{A}$ and the critical exponent β have been found to be 3.43 and 0.5028, respectively. Our critical exponent is therefore in excellent agreement (within a 0.6% error) with the experimental observation [10].

Although the above result agrees with the experimental observation extremely well, it is not unreasonable to suspect that our analysis can be in some way limited to only a small range above the transition threshold. After all, we have truncated the series expansions for the field components at the second-order in θ_0 for the sake of simplicity; the high order terms must play a role in the evolution of the normal rolls when the system is sufficiently far above the transition point. Knowing from experiment that the $\varepsilon^{1/2}$-dependence continues to hold true up to at least $\varepsilon = 0.1$ [10], we can determine the range in which our analysis applies by extending the bifurcation diagram until a significant departure from the experimental observation appears. The bifurcation diagram constructed over an extended range of ε is depicted in Figure 6, where it is clearly demonstrated that θ_0 begins to deviate from its $\varepsilon^{1/2}$-dependence and increase drastically as ε exceeds approximately 10^{-3}. The range of validity of our present analysis is therefore established.

While it is common to believe that formation of normal rolls corresponds to a second-order phase transition, our model suggests that these rolls could also be formed via a first-order transition. How this is indeed possible can be understood by plotting the fourth-order coefficient at the threshold i.e. $C_4(\bar{r}; V_c, \omega)$ as a function of the reduced frequency as shown in Figure 7. The figure shows that the critical value of C_4 is a decreasing function of ω' and becomes negative for ω' greater than a critical value $\omega_c' \approx 1.0345$. Just as the stability of the rest-state is dependent on the second-order coefficient, the order of transition depends on the fourth-order coefficient: the transition is continuous if C_4 is positive and discontinuous if C_4 is negative. Hence, from Figure 7, we infer that the transition line for the normal rolls is of second-order (supercritical) for ω' up to the critical value ω_c' and of first-order (subcritical) for $\omega' > \omega_c'$. In other words, there exists a tricritical point on the transition line at $\omega' = \omega_c'$. For the purpose of illustration, we have

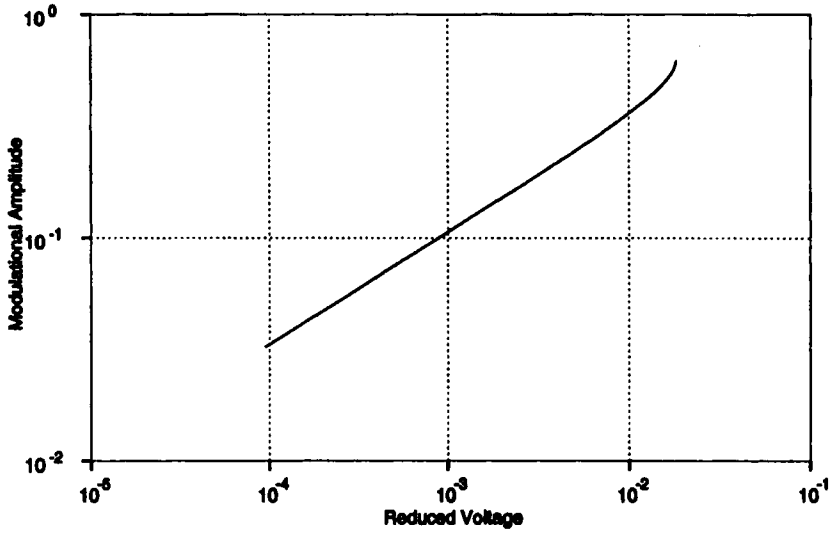

FIGURE 6 A log-log plot of the bifurcation diagram for θ_0 over an extended range of the reduced voltage ε.

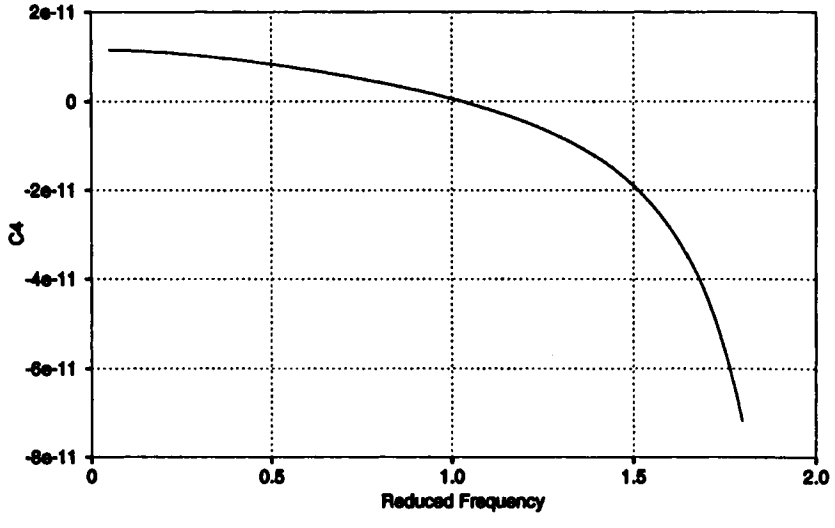

FIGURE 7 The value of C_4 at the transition point plotted as a function of the reduced frequency.

used the standard material parameters for MBBA to compute the curve for the critical C_4 in Figure 7. We have then found that the curve behaves qualitatively the same even if a non-standard value (1.15) for the conductivity ratio $\sigma_\parallel/\sigma_\perp$ is used. If we choose $\sigma_\parallel = 1.1895 \times 10^{-8}\Omega^{-1}\mathrm{m}^{-1}$, the above

critical value ω_c corresponds to the actual frequency $f_c = 46.84$ Hz. Since our fourth-order coefficient is only approximate, a precise determination of the location of this tricritical point is not possible at this time and hence the above critical value should only be taken as a rough estimate.

Interestingly, in a recent experiment designed to measure hydrodynamic fluctuations below the onset of a thin layer of a nematic liquid crystal, Rehberg *et al.* [39] have observed a subcritical bifurcation from the uniformly aligned state to the normal rolls at the driving frequency of 45 Hz. Although their observations are in favor of our theoretical predictions and their driving frequency is remarkably close to our approximate critical frequency (within 4.1%), further confirmation of our theory is not possible at this time since their experiment was performed at a fixed driving frequency and no other subcritical bifurcation of this kind at a different frequency has ever been reported.

6. CONCLUSIONS

The use of a generalized free energy description in nonequilibrium processes is still open to debate. Nevertheless, using a technique similiar to that proposed by Graham and Tél, we have found a functional from which the viscous torque due to the coupling between the director and the flow can be derived and, as a result, a nonequilibrium potential for the nematic cell is obtained. To describe the evolution of the normal rolls slightly above the transition threshold, we have gone beyond the linear approximation and obtained the first nonlinear corrections through the use of series expansions similar to the ε-expansions. Our results compare very favorably with experimental observations. Most notably, the bifurcation diagram deduced directly from the model has been found to agree with the experiment to within 0.6%. Although this result has a rather limited range of validity ($0 < \varepsilon < 0.001$) due to the early truncation of the series expansions of the field variables, the present model has an advantage over the amplitude description in that the $\varepsilon^{1/2}$-behavior near the threshold is a direct consequence of the model and is not an a priori assumption.

Finally, our model has yielded another important prediction in regard to the formation of normal rolls. Unlike earlier results due to the standard model (the linear and the weakly nonlinear analyses on the macroscopic deterministic equations of motion), the present model suggests that, at sufficiently high frequencies of the electric field, the regular straight rolls could be formed via a first-order transition. This prediction immediately points to

the presence of a tricritical point on the low-lying transition line. While discontinuous transitions from the rest-state to the oblique rolls have been commonly observed at low frequencies [8, 9, 40], a discontinuous transition from the rest-state to the normal straight rolls at a higher frequency has only been reported once so far [39]. Although the presence of a tricritical point cannot yet be substantiated due to the lack of experimental information, the possibility of forming normal rolls via a subcritical bifurcation has at least been verified.

From the theoretical point of view, the standard model predicts only a forward stationary (supercritical) bifurcation and no other method has yet implied subcritical bifurcations at the first transition thresholds. This puts our energy functional formalism in a very good perspective. The present approach allows one to see that the possibility of a subcritical bifurcation is due to the existence of local minima (metastable states) in the phenomenological free energy functional and thermal fluctuations are associated with fluctuations between these metastable states.

Acknowledgments

This research has been supported by the University of Alberta and by a grant from NSERC (Canada).

APPENDIX

Below, we explicitly list the coefficients found in the linear solutions (4.6)–(4.9) and the first nonlinear terms (4.12)–(4.15):

$$\bar{E}_{x1}(t) = -\frac{E_0}{g}[a\omega \sin(\omega t) + b \cos(\omega t)] \tag{A1}$$

$$\bar{v}_{x1} = \frac{E_0^2 r^2 d(\Delta\varepsilon - \tau\Delta\sigma)}{2\pi(\tau^2\omega^2 + 1)\xi} \tag{A2}$$

$$\bar{E}_{x2}(t) = A \sin(\omega t) + B \cos(\omega t) \tag{A3}$$

$$\bar{E}_{z2}(t) = \frac{E_0}{4g}\frac{(A_2\varepsilon_\perp + A_1\sigma_\perp)\omega \sin(\omega t) + (A_2\sigma_\perp - A_1\omega^2\varepsilon_\perp)\cos(\omega t)}{\sigma_\perp^2 + \omega^2\varepsilon_\perp^2} \tag{A4}$$

$$\bar{v}_{x2} = \frac{-q(A_x - A_z)}{8[p^4\eta_4 + q^4\eta_3 + p^2q^2(\eta_1 - \eta_2 - \eta_5)]} \tag{A5}$$

where

$$a = \Delta\sigma\tau - \Delta\varepsilon \tag{A6}$$

$$b = \Delta\varepsilon\tau\omega^2 + \Delta\sigma \tag{A7}$$

$$g = (\sigma_\parallel + \sigma_\perp r^2)(\tau^2\omega^2 + 1) \tag{A8}$$

$$\tau = (\varepsilon_\parallel + \varepsilon_\perp r^2)/(\sigma_\parallel + \sigma_\perp r^2) \tag{A9}$$

$$\xi = \eta_3 r^4 + (\eta_1 - \eta_2 - \eta_5)r^2 + \eta_4 \tag{A10}$$

$$\eta_1 = \alpha_1 + \alpha_4 + \alpha_5 + \alpha_6 \tag{A11}$$

$$\eta_2 = \frac{1}{2}(\alpha_4 + \alpha_6 - \alpha_3) \tag{A12}$$

$$\eta_3 = \frac{1}{2}(\alpha_3 + \alpha_4 + \alpha_6) \tag{A13}$$

$$\eta_4 = \frac{1}{2}(\alpha_4 + \alpha_5 - \alpha_2) \tag{A14}$$

$$\eta_5 = \frac{1}{2}(\alpha_5 - \alpha_4 + \alpha_2) \tag{A15}$$

$$A = \frac{qpE_0\omega}{2g}\left[\frac{A_1(\sigma_\perp q^2 + \sigma_\parallel p^2) + A_2(\varepsilon_\perp q^2 + \varepsilon_\parallel p^2)}{(\sigma_\perp q^2 + \sigma_\parallel p^2)^2 + \omega^2(\varepsilon_\perp q^2 + \varepsilon_\parallel p^2)^2}\right] \tag{A16}$$

$$B = \frac{qpE_0}{2g}\left[\frac{A_2(\sigma_\perp q^2 + \sigma_\parallel p^2) - A_1\omega^2(\varepsilon_\perp q^2 + \varepsilon_\parallel p^2)}{(\sigma_\perp q^2 + \sigma_\parallel p^2)^2 + \omega^2(\varepsilon_\perp q^2 + \varepsilon_\parallel p^2)^2}\right] \tag{A17}$$

$$A_1 = \Delta\sigma a + \Delta\varepsilon(g - b) \tag{A18}$$

$$A_2 = \Delta\sigma(b - g) + \Delta\varepsilon a\omega^2 \tag{A19}$$

$$A_x = \frac{pq}{2}\Bigg[(2\eta_5 + 4\eta_2 + 6\eta_3 - 4\eta_1)Aq - k_1 q^2 - \frac{aE_0^2\Delta\sigma}{2g} + 2(\eta_1 - \eta_2 - \eta_4)\frac{Ap}{r} - p^2(k_1 r^2 + 2k_3)\Bigg] \tag{A20}$$

$$A_z = -\frac{pqE_0^2}{4g^2}\{[5ab - (4bg + 3a^2\omega^2)\tau](\sigma_\parallel + \sigma_\perp r^2) + 4g^2\Delta\varepsilon\} - p^3[q(k_3 + k_1 r^2) + (\eta_1 - \eta_2 - 3\eta_4 - 2\eta_5)A] - pq^2 A(\eta_3 + \eta_5). \tag{A21}$$

References

[1] W. Helfrich, *J. Chem. Phys.*, **51**, 4092 (1969).
[2] E. F. Carr, *Mol. Cryst. and Liq. Cryst.*, **7**, 253 (1969).
[3] E. Dubois-Violette, P. G. de Gennes and O. Parodi, *J. Phys.*, (Paris), **32**, 305 (1971).
[4] P. A. Penz and G. W. Ford, *Phys. Rev.*, **A6**, 414 (1972).
[5] E. Bodenschatz, W. Zimmermann and L. Kramer, *J. Phys.*, (Paris), **49**, 1875 (1988).
[6] Orsay Liquid Crystals Group, *Phys. Rev. Lett.*, **25**, 1642 (1970).
[7] D. Meyerhofer and A. Sussman, *Appl. Phys. Lett.*, **20**, 337 (1972).
[8] R. Ribotta, A. Joets and L. Lei, *Phys. Rev. Lett.*, **56**, 1595 (1986).
[9] A. Joets and R. Ribotta, *J. Phys.*, (Paris), **47**, 595 (1986).
[10] S. Rasenat, G. Hartung, B. L. Winkler and I. Rehberg, *Experiments in Fluids*, **7**, 412 (1989).
[11] T. O. Carroll, *J. Appl. Phys.*, **43**, 1342 (1972).
[12] S. Kai, M. Araoka, H. Yamazaki and K. Hirakawa, *J. Phys. Soc. Jpn.*, **46**, 383 (1979).
[13] F. H. Busse, in *Cellular Structures in Instability* (Lecture Notes in Physics **210**), J. E. Wesfried and S. Zaleski, ed. (Springer, 1984), p. 97.
[14] D. Meyerhofer, in *Introduction to Liquid Crystals*, F. B. Priestley, P. J. Wojtowicz and P. Sheng, ed. (Plenum Press, New York, 1975), p. 129.
[15] W. Pesch and L. Kramer, *Z. Phys. B–Condensed Matter*, **63**, 121 (1986).
[16] V. L. Ginzburg and L. D. Landau, *Zh. Eksperim. i Teor. Fiz.*, **20**, 1064 (1950).
[17] C. Domb and M. S. Green, *Phase Transition and Critical Phenomena*, **5A**, 297 (1976).
[18] A. C. Newell and J. A. Whitehead, *J. Fluid Mech.*, **38**, 279 (1969).
[19] A. C. Newell, in *Nonlinear Wave Motion* (Lectures in Applied Mathematics), A. C. Newell, ed. (Americiam Mathematical Society, 1974), p. 157.
[20] L. Kramer and W. Zimmermann, *Physica*, **16D**, 221 (1985).
[21] A. Joets and R. Ribotta, *J. Stat. Phys.*, **64**, 981 (1991).
[22] H. Sakaguchi, *Prog. of Theor. Phys.*, **89**, 1123 (1993).
[23] H. Haken, in *Stochastic Nonlinear Systems*, L. Arnold and R. Lefever ed., (Springer-Verlag, Berlin, 1981), p. 12.
[24] R. Graham and H. Haken, *Z. Phys.*, **237**, 31 (1970).
[25] S. K. Chan, *J. Chem. Phys.*, **67**, 5755 (1977).
[26] J. S. Langer and V. Ambegaokar, *Phys. Rev.*, **164**, 498 (1967).
[27] D. E. McCumber, *Phys. Rev.*, **172**, 427 (1968).
[28] D. E. McCumber and B. I. Halperin, *Phys. Rev.*, **B1**, 1054 (1970).
[29] M. C. Cross and P. C. Hohenberg, *Rev. Mod. Phys.*, **65**, 851 (1993).
[30] R. Graham, in *Stochastic Nonlinear Systems*, L. Arnold and R. Lefever, ed., (Springer-Verlag, Berlin, 1981), p. 202.
[31] R. Graham and T. Tél, *Phys. Rev. Lett.*, **52**, 9 (1984), *J. Stat. Phys.*, **35**, 729 (1984), *Phys. Rev. A*, **31**, 1109 (1985), *Phys. Rev. A*, **33**, 1322 (1985), *Phys. Rev. A*, **35**, 1328 (1987).
[32] P. G. de Gennes and J. Prost, *The Physics of Liquid Crystals*, 2nd ed. (Clarendon Press, Oxford, 1993).

[33] F. C. Frank, *Faraday Soc. Disc.*, **25**, 19 (1958).
[34] O. Parodi, *J. Phys.*, (Paris), **31**, 581 (1970).
[35] P. C. Martin, O. Parodi and P. S. Pershan, *Phys. Rev.*, **A6**, 2401 (1972).
[36] F. M. Leslie, *Arch. Ration. Mech. Analaysis*, **28**, 265 (1968).
[37] W. Zimmermann and L. Kramer, *Phys. Rev. Lett.*, **55**, 402 (1985).
[38] W. H. Press, B. P. Flannery, S. A. Teukolsky and W. T. Vetterling, *Numerical Recipes in C* (Cambridge University Press, Cambridge, 1990), p. 305.
[39] I. Rehberg, S. Rasenat, M. de la Torre Juárez, W. Schöpf, F. Hörner, G. Ahlers and H. R. Brand, *Phys. Rev. Lett.*, **67**, 596 (1991).
[40] A. Joets and R. Ribotta, in *Cellular Structures in Instabilities*, edited by J. E. Wesfried, and S. Zaleski, (Springer-Verlag, New York, 1984), p. 294.